Calcium-induced Transitions between the Spontaneous Miniature Outward and the Transient Outward Currents in Retinal Amacrine Cells

Pratip Mitra and Malcolm M. Slaughter

Department of Physiology and Biophysics, School of Medicine, State University of New York at Buffalo, Buffalo, NY 14214

ABSTRACT Spontaneous miniature outward currents (SMOCs) occur in a subset of retinal amacrine cells at membrane potentials between −60 and −40 mV. At more depolarized potentials, a transient outward current (I_{to}) appears and SMOCs disappear. Both SMOCs and the I_{to} are K^+ currents carried by BK channels. They both arise from Ca^{2+} influx through high voltage–activated (HVA) Ca^{2+} channels, which stimulates release of internal Ca^{2+} from caffeine- and ryanodine-sensitive stores. An increase in Ca^{2+} influx resulted in an increase in SMOC frequency, but also led to a decline in SMOC mean amplitude. This reduction showed a temporal dependence: the effect being greater in the latter part of a voltage step. Thus, Ca^{2+} influx, although required to generate SMOCs, also produced a negative modulation of their amplitudes. Increasing Ca^{2+} influx also led to a decline in the first latency to SMOC occurrence. A combination of these effects resulted in the disappearance of SMOCs, along with the concomitant appearance of the I_{to} at high levels of Ca^{2+} influx. Therefore, low levels of Ca^{2+} influx, arising from low levels of activation of the HVA Ca^{2+} channels, produce randomly occurring SMOCs within the range of −60 to −40 mV. Further depolarization leads to greater activation of the HVA Ca^{2+} channels, larger Ca^{2+} influx, and the disappearance of discontinuous SMOCs, along with the appearance of the I_{to}. Based on their characteristics, SMOCs in retinal neurons may function as synaptic noise suppressors at quiescent glutamatergic synapses.

KEY WORDS: BK channels • ryanodine receptors • transient potassium current • ganglion cells • dihyropyridines

INTRODUCTION

Brief stochastic activations of clusters of large conductance Ca^{2+}-activated K^+ channels (BK channels) have been reported in certain neuronal cell types. These discrete events have been detected as spontaneous miniature hyperpolarizations (SMHs)* or spontaneous miniature outward currents (SMOCs) (Hartzell et al., 1977; Mathers and Barker, 1981, 1984; Brown et al., 1983; Satin and Adams, 1987; Fletcher and Chiappinelli, 1992; Merriam et al., 1999). Hartzell et al. (1977) reported membrane "noise" in amphibian neurons, which appeared as brief spontaneous hyperpolarizing potentials of a few millivolts. Although not studied in detail, it was suggested that they were due to changes in K^+ conductance. Subsequently, Mathers and Barker (1981, 1984) reported the presence of spontaneous discrete hyperpolarizing potentials at the resting membrane potential of cultured mouse dorsal root ganglion cells. These hyperpolarizations were the result of Ca^{2+}-dependent K^+ fluxes and, like synaptic potentials, had a fast rise and slower decay. They arose due to Ca^{2+} release from internal stores and appeared as outward currents when recorded under voltage clamp. Removal of bath Ca^{2+} resulted in their elimination, suggesting a requirement for Ca^{2+} influx for their activation. They were found to be sensitive to the membrane potential, with their amplitude and frequency decreasing with hyperpolarization and vice versa. SMOCs and SMHs have also been reported in bullfrog sympathetic neurons (Brown et al., 1983; Satin and Adams, 1987). Satin and Adams (1987) found that SMOCs in mudpuppy parasympathetic neurons and bullfrog sympathetic neurons arose due to intracellular Ca^{2+} release, but were not blocked by 200 μM Cd^{2+}, an inorganic blocker of voltage-gated Ca^{2+} channels (VGCCs). They concluded that Ca^{2+} influx was not necessary for SMOC generation. However, since SMOC frequency was voltage dependent, they hypothesized that cell depolarization was coupled to intracellular Ca^{2+} release.

Subsequently, Merriam et al. (1999) reported that Ca^{2+} influx through VGCCs was necessary for SMOC generation in mudpuppy parasympathetic neurons, even though SMOCs occurred in the presence of Cd^{2+},

Pratip Mitra's present address is Department of Neuroscience, University of Minnesota, 6-145 Jackson Hall, 321 Church St. SE, Minneapolis, MN 55455.

Address correspondence to Malcolm Slaughter, Department of Physiology and Biophysics, University at Buffalo, 124 Sherman Hall Buffalo, NY 14214. Tel.: (716) 829-3240; Fax: (716) 829-2344; E-mail: mslaught@buffalo.edu

*Abbreviations used in this paper: CICR, Ca^{2+}-induced Ca^{2+} release; DHP, dihydropyridine; HVA, high voltage–activated; SMH, spontaneous miniature hyperpolarization; sEPSP, spontaneous excitatory postsynaptic potential; SMOC, spontaneous miniature outward currents; STOC, spontaneous transient outward current; VGCC, voltage-gated Ca^{2+} channel.

 J. Gen. Physiol. © The Rockefeller University Press • 0022-1295/2002/04/373/16 $5.00
Volume 119 April 2002 373–388
http://www.jgp.org/cgi/content/full/119/4/373

albeit at a lower frequency. They found that SMOC generation in these neurons involved a process of Ca^{2+} influx that triggered Ca^{2+}-induced Ca^{2+} release (CICR), presumably analogous to the mechanism seen in cardiac cells. Although lowering Ca^{2+} influx into the cell lowered the frequency of SMOCs, their amplitude and other parameters were found to be largely unaffected.

As described in the preceding paper (Mitra and Slaughter, 2002, this issue), SMOCs in retinal amacrine cell neurons result from a sequence of events that includes Ca^{2+} influx through high voltage–activated (HVA) Ca^{2+} channels (including the L-type) and subsequent amplification by CICR (Mitra and Slaughter, 2002, this issue). However, a characteristic feature of these cells is that SMOCs in normal Ringer's appear exclusively within the narrow voltage range of −60 to −40 mV. Depolarization beyond −40 mV leads to disappearance of SMOCs, along with the appearance of a transient (I_{to}) and a sustained (I_{so}) outward K^+ currents. Since retinal SMOCs were shown to be K^+ currents and the recordings were made in quasiphysiological K^+ gradients (E_k = −95 mV), it is intriguing as to why they disappear at depolarized levels. It would be expected that depolarization, by providing a larger driving force for K^+, should enhance their amplitudes.

Experiments described here indicate that Ca^{2+} influx serves two roles: both to generate and to eliminate discrete SMOCs. At comparatively low levels of Ca^{2+} influx, such as would occur at negative membrane potentials or when VGCCs were partially blocked, discrete SMOCs are generated and have large amplitudes. However, when Ca^{2+} influx increases then SMOCs undergo a negative modulation of their amplitudes and a decrease in their first latency. As a consequence, discrete SMOCs disappear and a fast transient outward current (I_{to}) appears. Preliminary descriptions of initial aspects of this work have been presented previously (Mitra and Slaughter, 2000).

MATERIALS AND METHODS

The materials and procedures for this study are identical to those described in Mitra and Slaughter (2002, this issue). The retina of *Ambystoma tigrinum* was dissociated and acutely isolated neurons were used for the study. Neurons were held at −80 mV in normal Ringer's or that containing Co^{2+} (usually 6 mM), and SMOCs were elicited with repeated 500-ms depolarizing voltage steps. Since only bath calcium concentration was manipulated in this study, the notation "Ca^{2+}" used throughout the text refers to external calcium unless otherwise indicated. Data containing SMOCs were analyzed using Mini Analysis program (version 4.1.1; Synaptosoft, Inc.) and Origin (version 6.0; Microcal Software, Inc.). SMOCs were detected either using the automatic detection mode in the Mini Analysis software or manually by eye. Prior to SMOC detection, the value of the peak-positive deflection of the baseline current noise in the data group was set as a threshold. Generally, 30 sweeps of up to 500 ms duration were recorded from each cell and invariably 150–500 SMOCs were analyzed for each parameter. In experiments designed to test the first latency to SMOC occurrence, a minimum of 40 sweeps were analyzed under each condition.

To isolate calcium currents, the cells were bathed in an extracellular solution containing (in mM) 23 NaCl, 80 TEA, 2.5 KCl, 10 $CaCl_2$, 1 $MgCl_2$, 10 dextrose, and 5 HEPES, buffered to pH 7.8 with NaOH, and oxygenated. The internal pipette solution for such recordings contained (in mM) 40 K-gluconate, 70 TEA, 5 NaCl, 1 $MgCl_2$, 5 EGTA, 5 HEPES, and was adjusted to pH 7.4 with KOH. The pipette solution also contained an "ATP-regenerating cocktail" consisting of 4 mM ATP, 20 mM phosphocreatine, and 50 U/ml creatine phosphokinase. The voltage values stated have been corrected for pipette junction potential but not for series resistance. Data are expressed as mean ± SEM. Statistical differences were ascertained by Student's *t* test, where $P < 0.05$ was deemed significant.

RESULTS

Experiments were designed to test the Ca^{2+} and voltage dependence of various SMOC characteristics. The SMOC properties were: (a) SMOC frequency, (b) peak SMOC amplitude, and (c) first latency to SMOC occurrence.

SMOC Frequency

This section reports results of investigations determining the effects of depolarization and the extent of Ca^{2+} influx on SMOC frequency. To test the effect of Ca^{2+} influx on SMOC frequency, SMOCs were generated at a constant voltage of −10 mV in 6 mM Co^{2+} Ringer's containing increasing amounts of [Ca^{2+}]. As mentioned in the Mitra and Slaughter (2002, this issue), SMOCs were absent when bath Ca^{2+} was kept at nominal levels. However, increasing bath [Ca^{2+}] led to their appearance and a monotonic increase in frequency within the range tested. Fig. 1 A shows representative traces of SMOCs at 0.9 mM and 4.5 mM [Ca^{2+}]. A plot of SMOC frequency vs. [Ca^{2+}] from the same cell is shown in Fig. 1 B. The SMOC frequency at 0.9 mM [Ca^{2+}] was 7 ± 1.4 Hz. SMOC frequency increased with increased [Ca^{2+}], leading to a frequency of 54.2 ± 1.6 Hz at 4.5 mM [Ca^{2+}] ($P < 0.01$). In eight cells, average SMOC frequencies of 4.5 ± 0.7, 26.3 ± 2.9, and 44.4 ± 3.1 Hz were observed at 0.9, 2.7, and 4.5 mM [Ca^{2+}], respectively. These values are significantly different from each other at $P < 0.01$. All experiments described in this and subsequent sections, in which the bath [Ca^{2+}] was varied, gave results that were fully reversible.

These findings confirm a stimulatory role of [Ca^{2+}] on SMOC frequencies. They complement findings in Mitra and Slaughter (2002, this issue), showing that dihydropyridine (DHP) agonists and antagonists increase and decrease SMOC frequencies, respectively. In combination, they indicate that calcium influx regulates SMOC frequency. Although this stimulatory effect is apparent, it should be noted that moving to extremely high levels of bath [Ca^{2+}] leads to an apparent decrease in frequencies. This is due to negative modula-

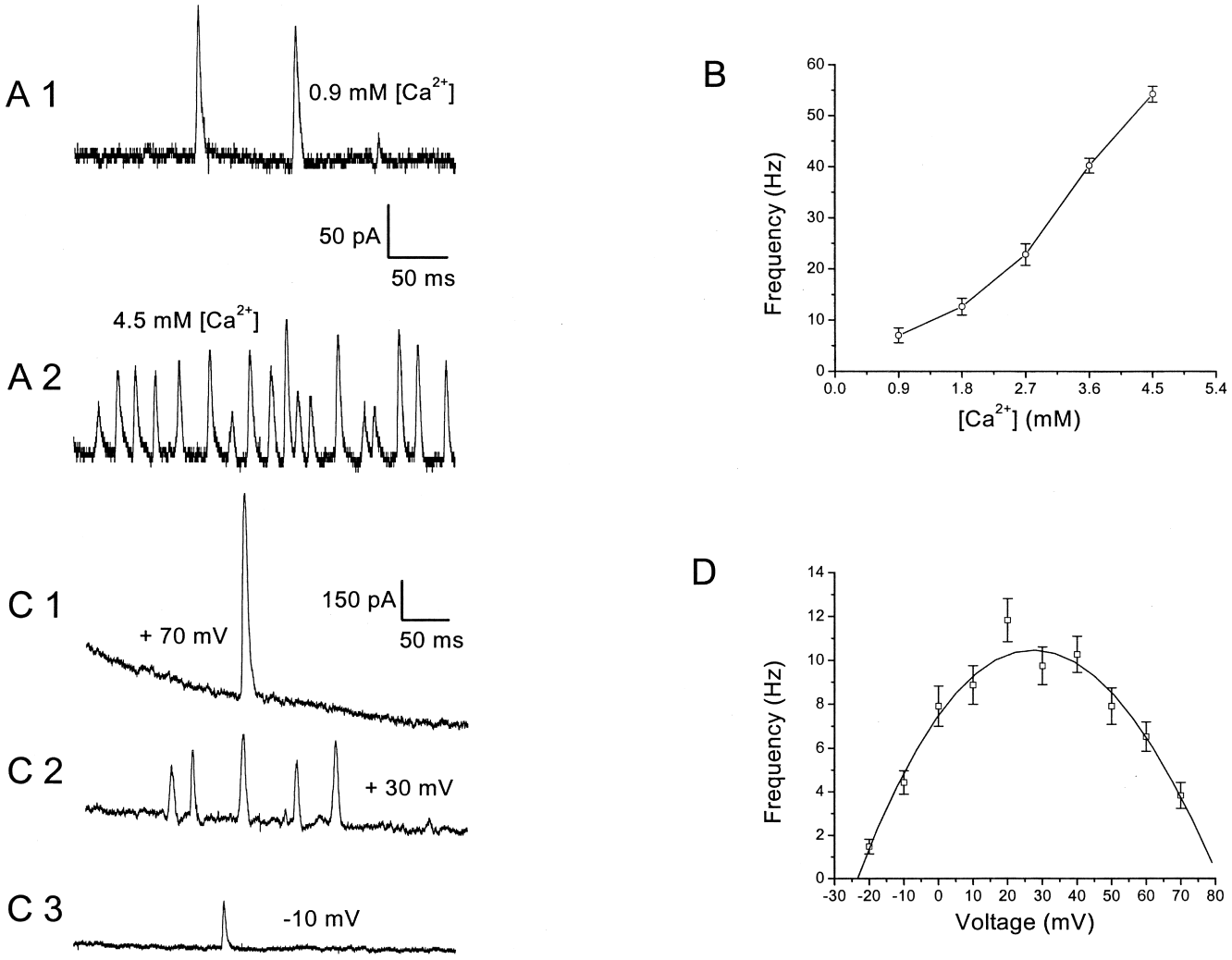

FIGURE 1. SMOC frequency increases with increasing Ca^{2+} influx. (A) SMOCs generated at −10 mV in 6 mM Co^{2+} Ringer's containing either 0.9 mM Ca^{2+} (A1) or 4.5 mM Ca^{2+} (A2). SMOCs were superimposed on a baseline current of ~65 pA. (B) Plot of SMOC frequency versus the extracellular Ca^{2+} concentration. Data generated from the same cell shown in A. (C) SMOCs generated in an amacrine cell at 70, 30, and −10 mV. SMOCs in C2 were superimposed on a baseline current of 670 pA, whereas those in C3 were on a current of 60 pA. The sag in trace C1 is presumably due to inactivation of the outward voltage–dependent current. In C1 the baseline current peaked at 1,493 pA and decayed to 841 pA at the end of the 500-ms pulse. (D) SMOCs were generated in 6 mM Co^{2+}/1.8 mM Ca^{2+} Ringer's by voltage steps from −20 to 70 mV in 10-mV increments in the same cell shown in C. Data shows the relationship between SMOC frequency and voltage. The smooth line through the data points depicts the biphasic nature of the relationship.

tion of SMOCs, which is seen at very high levels of Ca^{2+} influx and is described in subsequent sections.

In control Ringer's, SMOCs occurred over a narrow voltage range from −60 to −40 mV. However, when an inorganic HVA Ca^{2+} channel blocker (6 mM Co^{2+}) was present in the bathing solution, SMOCs were induced at voltages of −20 mV and above (Mitra and Slaughter, 2002, this issue). This afforded an opportunity to evaluate SMOCs over a much broader voltage range. To investigate the effects of voltage on SMOC frequency, SMOCs were generated in 6 mM Co^{2+}/1.8 mM Ca^{2+} Ringer's by a protocol which stepped cell voltage from −20 to 70 mV in 10-mV increments. Fig. 1 C shows representative SMOC recordings at 70, 30, and −10 mV. SMOCs were more frequent at the intermediate voltage of 30 mV as compared with either extreme. This cell had SMOC frequencies of 4.4 ± 0.5 Hz at −10 mV, 9.7 ± 0.9 Hz at 30 mV, and 3.8 ± 0.6 Hz at 70 mV. A plot of SMOC frequency at various voltages reveals a biphasic relationship (Fig. 1 D). The average SMOC frequencies in 10 cells under such conditions were 4.6 ± 0.4 Hz at −10 mV, 9.3 ± 0.7 Hz at 30 mV, and 3.9 ± 0.4 Hz at 70 mV. The frequency at 30 mV was significantly different from either extreme ($P < 0.01$). Such a biphasic effect of voltage on SMOC frequency has also been noted in other neuronal types (Satin and Adams, 1987; Merriam et al., 1999). The simplest interpretation

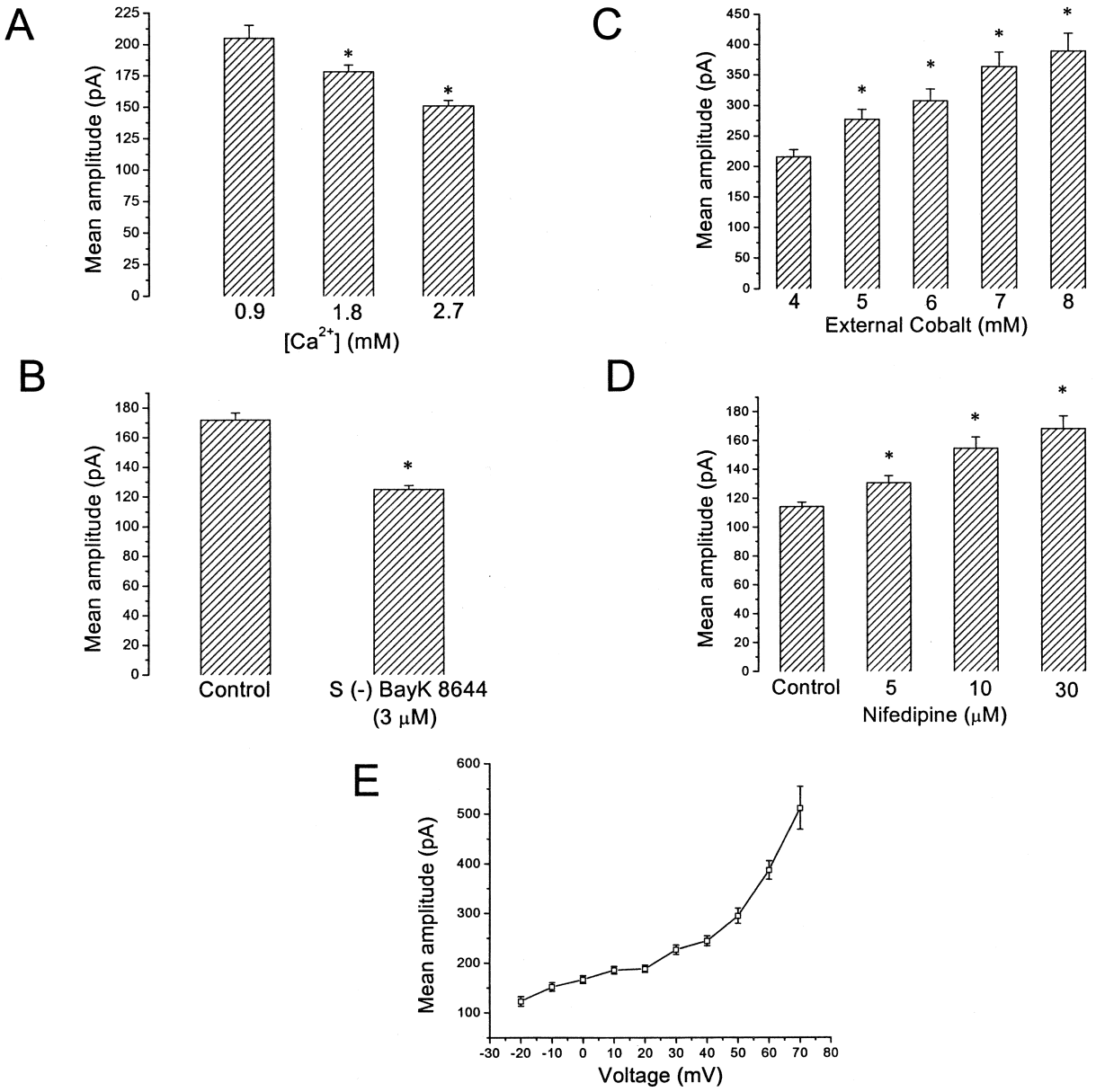

FIGURE 2. Increasing Ca^{2+} influx leads to a graded reduction in peak SMOC amplitudes. (A) Average data from seven cells showing reduction of peak SMOC amplitudes with increasing amounts of extracellular $[Ca^{2+}]$. SMOCs were generated in Ringer's containing 6 mM cobalt and varying amounts of Ca^{2+} (0.9–2.7 mM), with voltage steps to 30 mV. Asterisk indicates significance with reference to 0.9 mM $[Ca^{2+}]$. (B) S (−) BayK 8644 (3 μM), a DHP agonist, caused a statistically significant reduction of peak SMOC amplitudes ($P < 0.01$, $n = 6$). SMOCs were generated in 6 mM Co^{2+}/1.8 mM Ca^{2+} Ringer's with voltage steps to −10 mV. (C) SMOCs were generated by voltage steps to 30 mV with increasing amounts of Co^{2+} added to Ringer's containing 1.8 mM Ca^{2+}. Asterisk indicates a statistically significant difference with reference to 4 mM external cobalt ($P < 0.01$). (D) Mean peak SMOC amplitudes from a representative cell with increasing doses of the DHP antagonist, nifedipine. Control SMOCs were generated in 6 mM Co^{2+}/1.8 mM Ca^{2+} Ringer's with voltage steps to −10 mV. Asterisk indicates statistical significance at each dose with respect to control ($P < 0.05$). (E) I-V plot from a representative cell showing relationship between mean peak SMOC amplitudes and depolarization. SMOCs were generated in 6 mM Co^{2+}/1.8 mM Ca^{2+} Ringer's by steps from −20 to 70 mV in 10-mV increments.

of this response is that Ca^{2+} influx through VGCCs is biphasic. Ca^{2+} influx is governed by the channel open probability and the probability of unblock by cobalt, both of which increase with depolarization, and the calcium driving force, which decreases with depolarization.

Peak SMOC Amplitudes

Ca^{2+} influx affected SMOC amplitude as well as frequency. SMOCs were generated at 30 mV in 6 mM Co^{2+} Ringer's solution containing increasing amounts of

[Ca^{2+}] and peak SMOC amplitudes were determined. Fig. 2 A is a plot of average SMOC amplitudes at various [Ca^{2+}] obtained from seven cells, showing that peak amplitudes declined in a graded manner as bath [Ca^{2+}] increased. SMOCs under these conditions had peak amplitudes of 204.9 ± 10.4 pA, 178 ± 5.4 pA, and 150.8 ± 4.3 pA in 0.9, 1.8, and 2.7 mM [Ca^{2+}], respectively. These values are significantly different from each other, with the value at 2.7 mM being different from that obtained at 0.9 mM at $P < 0.01$. This suggests that Ca^{2+} influx causes a graded reduction in the mean peak SMOC amplitudes.

Since it was shown in the preceding paper that Ca^{2+} influx through L-type VGCCs is involved in SMOC generation, an L-type Ca^{2+} channel agonist would be expected to increase Ca^{2+} influx and lower peak SMOC amplitudes. SMOCs were generated at −10 mV in 6 mM Co^{2+}/1.8 mM Ca^{2+} Ringer's solution. Addition of the DHP agonist, S (−) BayK 8644 (3 μM), decreased mean peak SMOC amplitudes. The effects of the agonist described in this and subsequent sections could not be washed out on returning to control solution. Average data from six cells is shown in Fig. 2 B, in which the mean amplitude decreased from 171.8 ± 4.8 pA in control to 124.8 ± 2.7 pA with the agonist ($P < 0.01$). This indicates that Ca^{2+} influx, which is required for SMOC generation, suppresses SMOC amplitude.

If increased Ca^{2+} influx results in a decrease in mean peak SMOC amplitudes, then reduction of Ca^{2+} influx should result in an increase. Experimentally, Ca^{2+} influx was reduced either by addition of the DHP antagonist nifedipine, or by increasing amounts of bath Co^{2+}. Fig. 2 C shows results from a cell in which SMOCs were generated at 30 mV while increasing amounts of cobalt were added to Ringer's containing 1.8 mM Ca^{2+}. The mean SMOC amplitude in this cell was 215 ± 12 pA when 4 mM Co^{2+} was present in the bath solution. Increasing the Co^{2+} to 8 mM raised the mean amplitude reversibly to 389 ± 29 pA ($P < 0.01$). In eight cells, mean SMOC amplitudes were 182.5 ± 5 pA and 244.8 ± 12.7 pA in 4 and 8 mM Co^{2+}, respectively ($P < 0.01$). Reduction of Ca^{2+} influx by nifedipine gave similar results ($n = 18$). A representative data plot is shown in Fig. 2 D. The mean peak SMOC amplitude in this cell, for control SMOCs generated at −10 mV in 6 mM Co^{2+}/1.8 mM Ca^{2+} Ringer, was 114 ± 3 pA. Nifedipine caused a dose-dependent increase in the mean amplitude, raising it to 168 ± 9 pA at 30 μM ($P < 0.01$). Average data from seven cells in which SMOCs were generated at 30 mV in 6 mM Co^{2+}/1.8 mM Ca^{2+} Ringer's gave a mean amplitude of 216.5 ± 5.2 pA. Amplitude increased to 304.7 ± 11.9 pA and 332.8 ± 16.6 pA with addition of 10 and 30 μM nifedipine, respectively ($P < 0.01$). The effects of nifedipine described here and in subsequent sections were partially reversible on washout of the drug. The lack of reversibility seen with DHPs is perhaps due to their lipid solubility, which results in uptake into membranes (Pang and Sperelakis, 1984; Nerbonne and Gurney, 1987), particularly when high doses were used.

These results reveal that SMOCs are negatively modulated by Ca^{2+}, whereby an increase in its influx causes a decrease in peak SMOC amplitude. Conversely, reducing Ca^{2+} influx is equivalent to removal of the negative modulation, as shown by the increase in the peak amplitudes obtained either by nifedipine or elevated Co^{2+}.

In the same set of data that was used to study the effect of voltage on SMOC frequency, variation of SMOC amplitudes with the level of depolarization was examined. Fig. 2 E shows an I-V plot for SMOCs obtained from a representative cell. There is an increase in peak SMOC amplitude with depolarization. The mean SMOC amplitude at −10 mV is 152 ± 8 pA. The amplitude increased to 227 ± 9 pA at 30 mV and to 511 ± 43 pA at 70 mV. Average data from 10 cells gave mean SMOC amplitudes of 148.7 ± 5.4 pA, 237.1 ± 6.1 pA, and 541.1 ± 23.1 pA at −10, 30, and 70 mV respectively (values are significantly different from each other at $P < 0.01$). It should be noted that the gradient of the curve in Fig. 2 E is not constant along the voltage axis. Although increasing relatively linearly from −20 to 40 mV, it tends to show an increase in slope beyond 40 mV. Since SMOCs are K^+ currents, a linear increase in peak amplitude with depolarization is explained as an increased driving force for K^+ ions. The reason for the increase in slope above 40 mV was not determined. It may reflect a pure voltage dependence of SMOCs, or it may be due to removal of the Ca^{2+}-induced negative modulation of SMOCs at very depolarized voltages (see DISCUSSION).

Temporal Dependence of SMOC Amplitudes

Although increased Ca^{2+} influx reduced peak SMOC amplitudes, this reduction was greater for SMOCs occurring in the latter half of a 500 ms depolarizing voltage step. This temporal dependence becomes significant at higher [Ca^{2+}]. Fig. 3 A shows representative traces for SMOCs generated with 500-ms steps to 30 mV in the presence of 6 mM Co^{2+} Ringer's containing 0.9 or 2.7 mM Ca^{2+}. The double-headed arrows mark the midpoint of the 500-ms voltage steps. In 2.7 mM [Ca^{2+}], SMOCs elicited in the latter 250 ms (β) are on the average smaller in peak amplitude as compared with those seen in the first half of the step (α). Such a temporal dependence is not obvious with SMOCs generated in 0.9 mM [Ca^{2+}]. Fig. 3 B is a plot from the same cell of mean SMOC amplitudes in the first and second 250-ms intervals of the voltage step, as ascertained under different [Ca^{2+}]. It illustrates the temporally dependent reduction of am-

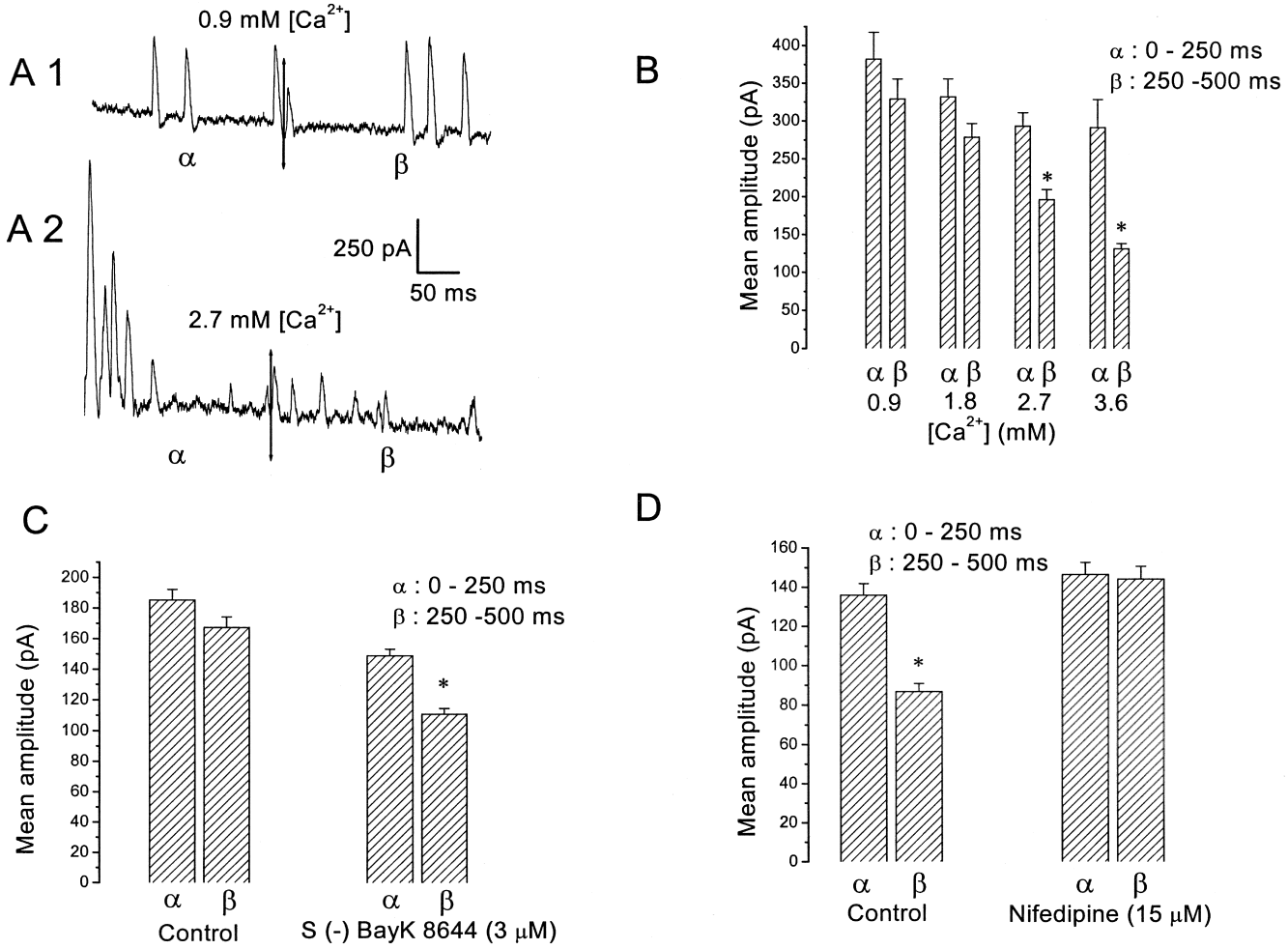

FIGURE 3. Temporal properties of SMOC amplitudes. (A) SMOCs generated by 500-ms steps to 30 mV in 6 mM Co^{2+} Ringer's containing either 0.9 mM Ca^{2+} or 2.7 mM Ca^{2+}. The double-headed arrows in both traces separate the first 250 ms of the voltage step (α) and the second 250 ms (β). The notation α and β are used with the same meaning in the other panels. SMOCs in this cell were superimposed on a baseline current of ~900 pA. (B) Data plot from the same cell showing mean peak SMOC amplitudes in the two intervals of the 500-ms voltage step. Asterisk indicates statistically significant difference in β as compared with α ($P < 0.01$). (C) Effect of DHP agonist, S (−) BayK 8644 (3 μM), on peak SMOC amplitudes in α and β intervals. SMOCs were generated in 6 mM Co^{2+}/1.8 mM Ca^{2+} Ringer's with steps to −10 mV. Asterisk indicates statistically significant between α and β ($P < 0.01$). Data is an average of six cells. (D) The DHP antagonist, nifedipine (15 μM), eliminates the temporal dependence of SMOC amplitudes. Control SMOCs were generated at 30 mV in 6 mM Co^{2+}/2.7 mM Ca^{2+} Ringer's, conditions which significantly lowered SMOC amplitude in the latter part (β) of the pulse (asterisk indicates $P < 0.01$). Nifedipine eliminates this temporal dependence ($P > 0.05$). Data is an average of five cells.

plitudes, with statistically significant reductions obtained for SMOCs generated in 2.7 and 3.6 mM [Ca^{2+}] ($P < 0.01$). The mean SMOC amplitude in this cell elicited with 3.6 mM [Ca^{2+}] in the first 250 ms of the pulse (α) was 291 ± 37 pA, and was reduced by ~55% to 132 ± 7 pA in the latter half of the pulse (β). Average data from seven cells yielded mean peak SMOC values of 277.8 ± 27 pA (α) and 312.8 ± 30.9 pA (β) under 0.9 mM [Ca^{2+}], values which are not significantly different at $P < 0.05$. But increasing [Ca^{2+}] to 2.7 mM gave values of 255.9 ± 12.8 pA (α) and 129.7 ± 4.9 pA (β); a reduction of ~50% in the latter half of the pulse ($P < 0.01$).

Regulation of Ca^{2+} influx by dihydropyridines gave similar results. Increasing Ca^{2+} influx by S (−) BayK 8644 (3 μM) led to an increase in the temporal dependence of peak SMOC amplitudes (Fig. 3 C). Control SMOCs generated at −10 mV in 6 mM Co^{2+}/1.8 mM Ca^{2+} Ringer's did not show a significant temporal dependence. Control SMOCs had mean amplitudes of 185 ± 7 pA (α) and 167 ± 7 pA (β), not significantly different at $P < 0.05$ ($n = 6$). Addition of S (−) BayK 8644 (3 μM) generated SMOCs with mean amplitudes of 149 ± 4 pA (α) and 111± 4 pA (β); a reduction of ~25% in the latter 250 ms ($P < 0.01$). Reducing Ca^{2+} influx with nifedipine had the opposite effect, eliminat-

ing the temporal dependence. Control SMOCs were generated at 30 mV in 6 mM Co^{2+} and 2.7 mM Ca^{2+} Ringer's, since peak SMOC amplitudes show a temporal dependence at this calcium concentration. Addition of 15 μM nifedipine eliminated this temporal dependence. Average data from five cells is shown in Fig. 3 D. Mean peak SMOC amplitudes under control conditions were 135.9 ± 6 pA (α) and 86.7 ± 4.1 pA (β), an ~37% reduction in the latter part of the pulse ($P <$ 0.01). SMOCs obtained in nifedipine had mean amplitudes of 146.6 ± 6 pA (α) and 144.3 ± 6.5 pA (β); this difference was not significant at $P < 0.05$. Increasing doses of Co^{2+} had a similar effect as nifedipine ($n = 8$; unpublished data). These results reveal a temporal dependence to the Ca^{2+} influx-induced negative modulation of SMOCs.

In addition to modulation of SMOC amplitudes, SMOC decay characteristics were modulated by Ca^{2+} influx in a qualitatively parallel manner. Experimental conditions that permitted greater Ca^{2+} influx resulted in SMOCs that decayed faster (measured as the time required to decay to 50% of peak or $t_{1/2}$). This reduction in decay time was graded with the extent of influx. Average data from seven cells in which SMOCs were generated at 30 mV in 6 mM Co^{2+} Ringer's containing varying amounts of [Ca^{2+}] gave $t_{1/2}$ values of 3.26 ± 0.09, 3.01 ± 0.06, and 2.86 ± 0.06 ms at 0.9, 1.8, and 2.7 mM [Ca^{2+}], respectively (values are significantly different at $P < 0.05$ with respect to 0.9 mM [Ca^{2+}]). Increasing Ca^{2+} influx by addition of the DHP agonist resulted in SMOCs that were more transient. Average data from six cells in which SMOCs were generated at −10 mV in 6 mM Co^{2+}/1.8 mM Ca^{2+} Ringer's gave $t_{1/2}$ values of 3.09 ± 0.08 ms (control) and 2.84 ± 0.06 ms (3 μM S [−] BayK 8644). These values are significantly different from each other at $P < 0.05$. Reducing Ca^{2+} influx with nifedipine gave opposite results. Average data from seven cells in which SMOCs were generated at 30 mV in 6 mM Co^{2+}/1.8 mM Ca^{2+} Ringer's gave $t_{1/2}$ values of 3.12 ± 0.09 ms (control), 3.92 ± 0.17 ms (10 μM nifedipine), and 4.42 ± 0.22 ms (30 μM nifedipine). These values are significantly different from control at $P <$ 0.01. Reducing Ca^{2+} influx into the cell by depolarizing the cell to very positive potentials produced similar results. SMOCs generated at −10 mV were more transient as compared with those generated at 70 mV. Average data from 10 cells gave $t_{1/2}$ values of 3.73 ± 0.12, 3.85 ± 0.1, and 6.24 ± 0.25 ms at −10, 30, and 70 mV, respectively. The value obtained at 70 mV is significantly different from −10 mV at $P < 0.01$. It is not possible to ascertain via our experiments whether the slowing of decay at extremely positive voltages is an inherently voltage-dependent feature, or if it is a consequence of reduction of Ca^{2+} influx. It is likely to be a combination of both. The biphasic nature of Ca^{2+} influx into the cell through VGCCs might account for the fact that the $t_{1/2}$ at 30 mV is not significantly different from that at −10 mV. Similar to SMOC amplitudes, the 50% decay times of SMOCs showed a temporal dependence under conditions of increased influx. SMOCs generated in the latter part of the pulse were more transient as compared with those generated in the initial part. Average data from seven cells gave $t_{1/2}$ values of 3.77 ± 0.22 ms (α; 0–250 ms) and 4.11 ± 0.29 ms (β; 250–500 ms) with 6 mM Co^{2+}/0.9 mM Ca^{2+} Ringer's. These values are not significantly different at $P < 0.05$. However, in 6 mM Co^{2+}/2.7 mM Ca^{2+} Ringer's, $t_{1/2}$ values of 3.61 ± 0.13 ms (α) and 2.68 ± 0.12 ms (β) were obtained (significantly different at $P < 0.01$). Increasing Ca^{2+} influx into the cell via addition of 3 μM of the DHP agonist ($n = 6$) introduced a temporal dependence in the decay times, whereas reduction of influx via addition of the antagonist nifedipine (15 μM; $n = 5$) or increasing doses of Co^{2+} ($n =$ 8) eliminated it (unpublished data).

First Latency to SMOC Occurrence

Another parameter examined for its Ca^{2+} and voltage dependence was the first latency to SMOC occurrence. It is defined as the average time that elapses after the onset of the voltage clamp step, before detection of the first SMOC. SMOCs were generated at −10 mV in 6 mM Co^{2+} Ringer's containing varying amounts of [Ca^{2+}], and the mean first latency to their occurrence was measured. Fig. 4 A shows representative traces generated at 0.9, 1.8, and 2.7 mM [Ca^{2+}]. The mean first latencies from this cell are plotted in Fig. 4 B as a function of [Ca^{2+}]. There is a graded decrease in the mean first latency to SMOC occurrence as [Ca^{2+}] increased. The mean first latency in this cell is 189 ± 37.3 ms at 0.9 mM [Ca^{2+}], and it decreases to 21.3 ± 4.6 ms at 2.7 mM [Ca^{2+}] ($P < 0.01$). Further increase to 3.6 mM [Ca^{2+}] leads to a value of 7.4 ± 1.3 ms, suggesting that at these high levels of influx, the delay to appearance of the first SMOC is extremely small. Average data from six cells gave a mean first latency value of 204.2 ± 24.5 ms at 0.9 mM [Ca^{2+}], which decreased to 52.3 ± 9.3 ms at 2.7 mM [Ca^{2+}] ($P < 0.01$).

Increasing Ca^{2+} influx by addition of the DHP agonist, S (−) BayK 8644 (3 μM), also led to a decrease in the mean first latency to SMOC occurrence ($n =$ 6). Average data from six cells in which control SMOCs were generated at −10 mV in 6 mM Co^{2+}/1.8 mM Ca^{2+} Ringer's are shown in Fig. 4 C. The mean first latency was reduced from 139.6 ± 17.3 ms (control) to 36.4 ± 5.2 ms by the agonist ($P < 0.01$). Conversely, decreasing Ca^{2+} influx either via addition of 10 μM nifedipine ($n = 7$; Fig. 4 D) or increasing doses of the inorganic blocker Co^{2+} ($n = 8$; unpublished data), led to an increase in the mean first la-

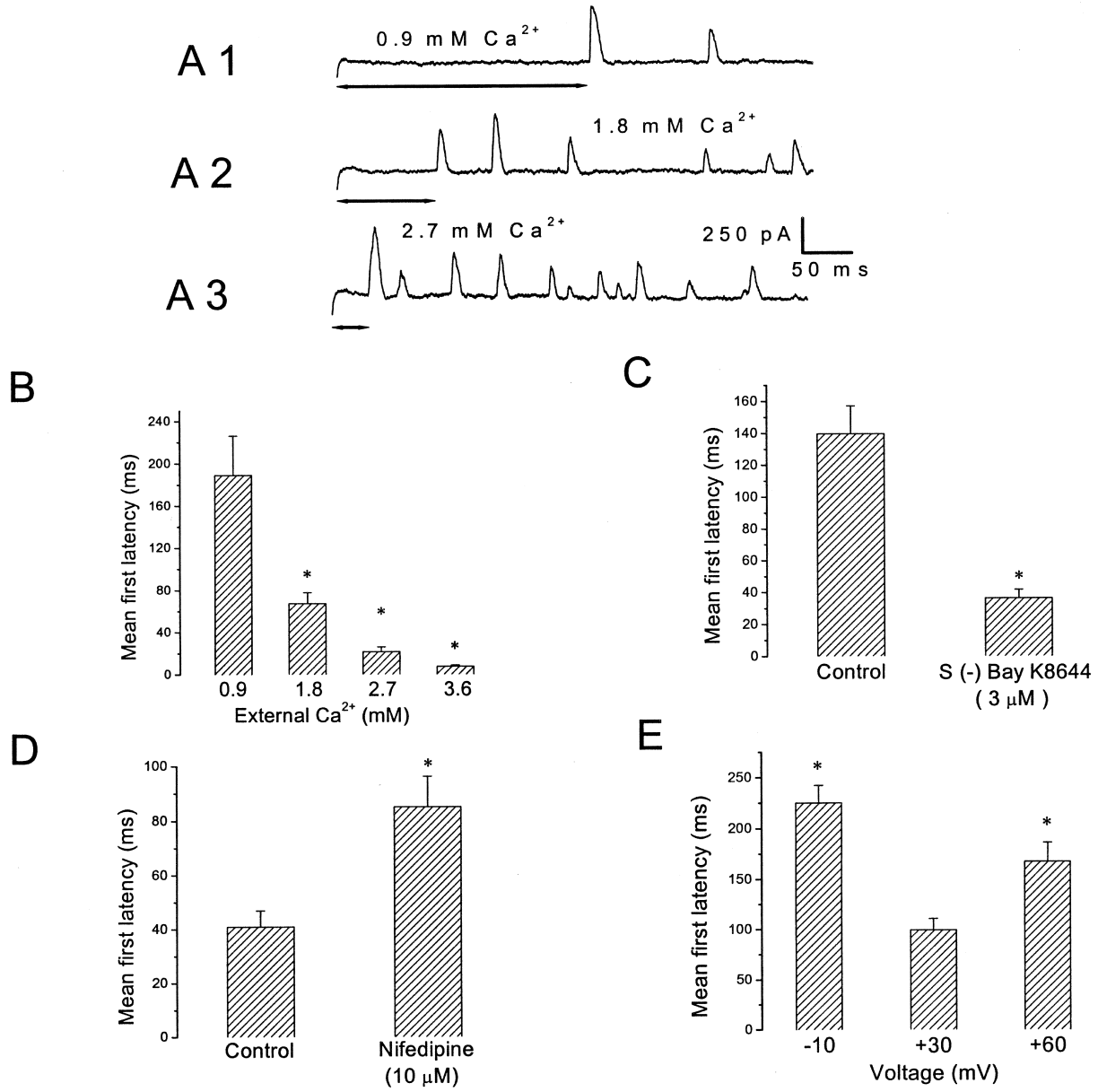

FIGURE 4. First latency to SMOC occurrence. (A) SMOCs generated at −10 mV in 6 mM Co^{2+} Ringer's containing either 0.9 mM (A 1), 1.8 mM (A 2), or 2.7 mM (A 3) $[Ca^{2+}]$. The double-headed arrows indicate the first latency to occurrence. Baseline current was ~130 pA. (B) Average first latency values from the same cell. Asterisks indicate values significantly lower than at 0.9 mM $[Ca^{2+}]$ ($P < 0.01$). (C) Mean first latency for SMOCs generated at −10 mV in 6 mM Co^{2+}/1.8 mM Ca^{2+} Ringer, showing that 3 μM S (−) BayK 8644 decreased first latency (asterisk indicates $P < 0.01$). Data are the average of six cells. (D) Nifedipine (10 μM) significantly increased the first latency as compared with control (asterisk indicates $P < 0.01$). Data are average of seven cells. SMOCs were generated in 6 mM Co^{2+}/1.8 mM Ca^{2+} Ringer's by steps to 30 mV. (E) Effect of cell voltage on first latency to SMOC occurrence. SMOCs were generated in 6 mM Co^{2+}/1.8 mM Ca^{2+} Ringer's by voltage steps to −10, 30, and 60 mV. Asterisks indicate that the first latency values at −10 and 60 mV were significantly different from that obtained at 30 mV ($P < 0.01$). Data are an average of 10 cells.

tency to SMOC occurrence. Control SMOCs were generated in 6 mM Co^{2+}/1.8 mM Ca^{2+} Ringer's with voltage steps to 30 mV (average data from seven cells; Fig. 4 D). There is an increase in the mean first latency to SMOC occurrence with 10 μM of the antagonist (control: 40.9 ± 6 ms; nifedipine: 85.1 ± 11 ms; $P < 0.01$). The common inference drawn from these observations is that increasing the probability of Ca^{2+} influx into the cell decreases the mean first latency to SMOC occurrence.

First latency values were found to be biphasic with voltage when SMOCs were generated at different voltage levels with a constant $[Ca^{2+}]$. SMOCs were generated in 6 mM Co^{2+}/1.8 mM Ca^{2+} Ringer's by a protocol

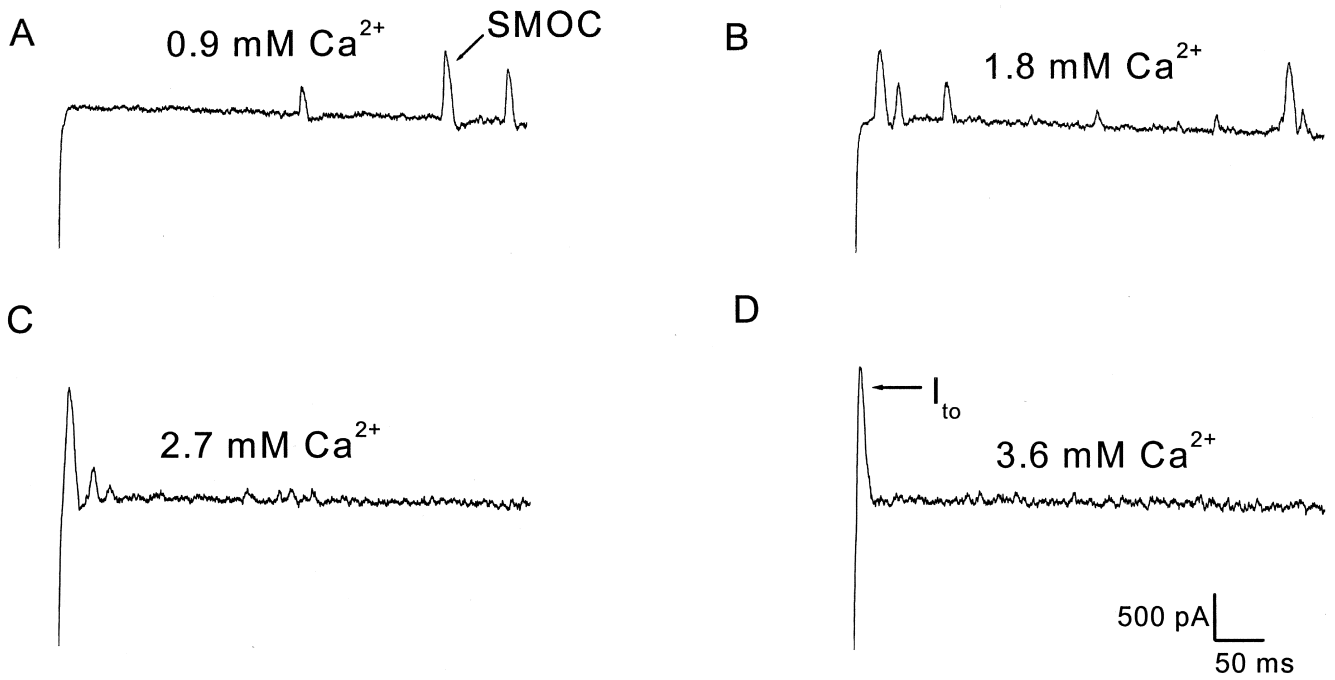

FIGURE 5. Ca^{2+} influx induced transition between SMOCs and the I_{to}. Cells were bathed in 6 mM Co^{2+}/1.8 mM Ca^{2+} Ringer's and currents were elicited by depolarizing steps to 30 mV. SMOCs superimposed on a voltage-induced outward current of ~1900 pA. Traces were from a representative cell in 0.9 (A), 1.8 (B), 2.7 (C), and 3.6 (D) mM [Ca^{2+}]. Note the gradual disappearance of SMOCs and the concomitant appearance of a transient outward K^+ current (I_{to}).

in which the voltage was stepped to −10, 30, and 60 mV. Average first latency values obtained from 10 cells are shown in Fig. 4 E. SMOCs at −10 mV appeared with a mean first latency of 225.2 ± 17 ms. Subsequent depolarization to 30 mV decreased mean first latency to 99.3 ± 11.3 ms. However, further depolarization to 60 mV lead to an increase in the mean first latency (167.4 ± 18.6 ms). The values at −10 and 60 mV were significantly different from the first latency observed at 30 mV ($P < 0.01$).

The Ca^{2+}-induced Transition of SMOCs into the I_{to}

The results presented thus far suggest a Ca^{2+} influx dependence of SMOCs, whereby increasing influx lead to a temporally dependent reduction in peak amplitude and first latency of SMOC occurrence. An extreme consequence of these effects is that at high levels of Ca^{2+} influx individual SMOCs disappear, with the concomitant appearance of the transient outward K^+ current (I_{to}). This occurs in a gradual fashion as influx increased (Fig. 5). Cells were bathed in 6 mM Co^{2+} Ringer's containing varying amounts of [Ca^{2+}] (0.9, 1.8, 2.7, 3.6, and 4.5 mM) and pulsed to 30 mV. Fig. 5 A is a trace from a representative cell in 0.9 mM [Ca^{2+}]. Individual SMOCs are clearly evident. However, increasing bath [Ca^{2+}] caused a gradual disappearance of individual SMOCs along with the appearance of the I_{to}. In this cell, at 3.6 mM [Ca^{2+}], individual SMOCs completely disappear, leaving the I_{to} (Fig. 5 D). In a total of eight cells studied at 30 mV, three cells displayed a total disappearance of SMOCs and generated the I_{to} by 3.6 mM [Ca^{2+}], whereas in the rest SMOCs disappeared at 4.5 mM [Ca^{2+}]. Thus, increasing levels of Ca^{2+} influx into the cells causes a gradual disappearance of discrete SMOCs along with the appearance of the I_{to}.

It is difficult to conclude from our recordings whether the I_{to} is a summation of individual SMOCs or is a single event. Individual SMOCs measured at 30 mV under 6 mM Co^{2+}/0.9 mM Ca^{2+} Ringer, had mean amplitudes equivalent to 46 ± 6% of the amplitude of I_{to} generated at that voltage under 6 mM Co^{2+}/3.6 or 4.5 mM Ca^{2+} Ringer's (values are averages from five cells). These values would argue against a summation theory, since they would suggest that the average I_{to} is comprised of only two SMOC events. However, since SMOCs undergo a Ca^{2+}-induced negative modulation of their amplitudes, the I_{to} may be a summation of many SMOCs whose amplitudes are far lower than those estimated at 0.9 mM [Ca^{2+}].

Individual SMOCs and the I_{to} Show Similar Pharmacological Sensitivities

The results indicate that I_{to} is formed from SMOCs. It was shown in the previous paper that both SMOCs and the I_{to} were Ca^{2+} influx–sensitive. SMOCs are K^+

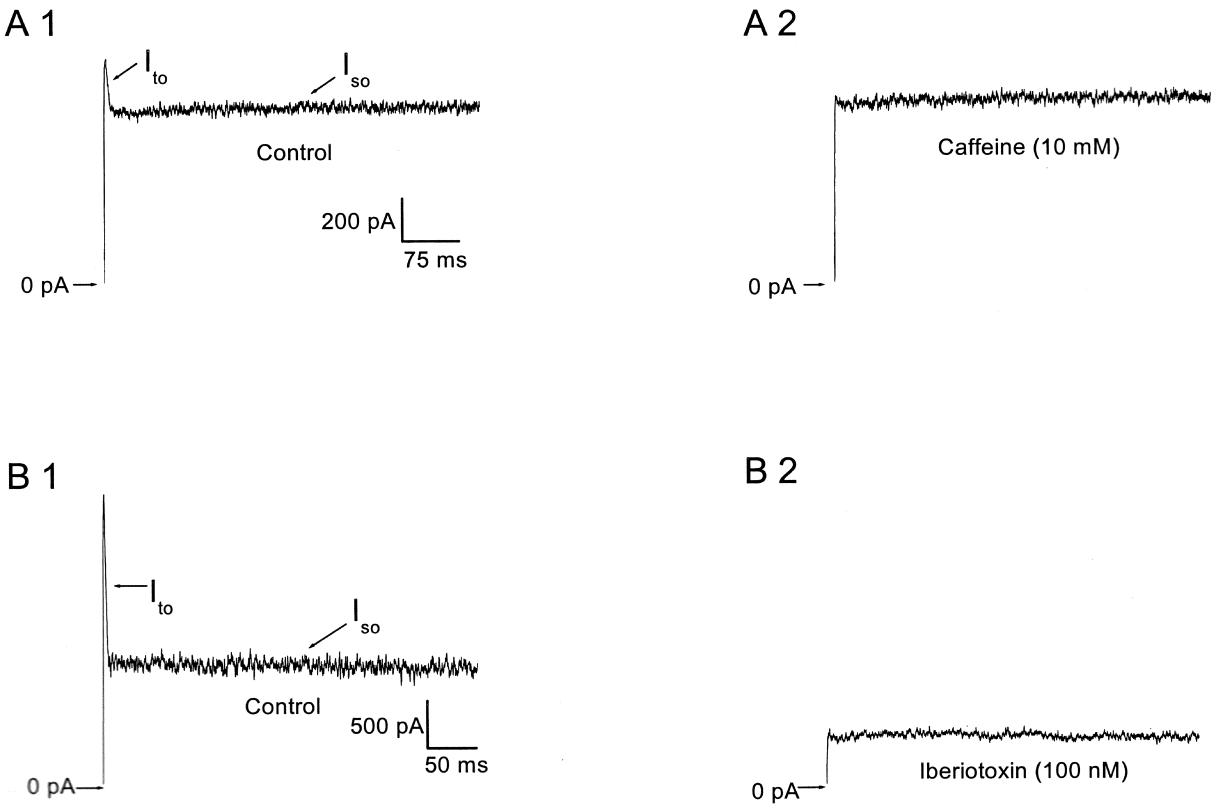

FIGURE 6. Pharmacological sensitivity of the I_{to}. (A1) Representative control trace generated in normal Ringer's at 10 mV shows the I_{to}. (A2) Addition of 10 mM caffeine selectively eliminated the I_{to}. (B1) Representative control trace generated at −30 mV shows the I_{to}. (B2) Addition of 100 nM iberiotoxin eliminated I_{to} in addition to reducing the sustained component, I_{so}. Recordings were made in normal Ringer's containing 0.1% wt/vol bovine serum albumin.

currents through BK channels and are insensitive to apamin but blocked by TEA and iberiotoxin. They are also dependent on CICR from caffeine- and ryanodine-sensitive stores (Mitra and Slaughter, 2002, this issue). If SMOCs lead to the I_{to}, it follows they should have similar pharmacological sensitivities. Fig. 6 presents data supporting this hypothesis. Similar to SMOCs, the I_{to} was eliminated on depletion of intracellular stores with 10 mM caffeine ($n = 10$). Fig. 6 A1 shows recordings in normal Ringer's from a representative cell with a voltage step to 10 mV. Addition of 10 mM caffeine results in a selective elimination of the I_{to} (A2). The effects of caffeine were fully reversible on washout of the drug. 10 mM caffeine selectively blocked the I_{to} generated by depolarizations up to 10 mV while leaving the sustained outward current, I_{so}, unchanged. However, at more depolarized levels such as 50 or 70 mV, 10 mM caffeine did reduce the I_{so} in addition to eliminating the I_{to}. This is presumably because caffeine at these doses is known to block the delayed rectifier K^+ current, the inhibition being greater at more depolarized voltages (Reiser et al., 1996). Recordings in normal Ringer's with 200 μM ryanodine in the internal pipette solution also led to an elimination of the I_{to} at all voltages at which it appears ($n = 6$; unpublished data). This finding, combined with the effect of store depletion by caffeine, suggests that CICR generates I_{to} as well as SMOCs.

The I_{to} was also eliminated when neurons were exposed to iberiotoxin, a blocker of BK channels (Fig. 6 B). Iberiotoxin, while eliminating the I_{to} at all voltages at which it appears, also suppressed I_{so} ($n = 7$). The I_{so} was reduced by 43 ± 3% at −10 mV (mean from six cells) in the presence of iberiotoxin. The effects of iberiotoxin were not reversible. In the preceding paper (Mitra and Slaughter, 2002, this issue), it was shown that the I_{so} is composed of two components, namely a Ca^{2+}-dependent $I_{so\text{-}Ca}$ and the Ca^{2+}-insensitive $I_{so\text{-}v}$ (Mitra and Slaughter, 2002, this issue). It is probable that the $I_{so\text{-}Ca}$, similar to SMOCs and the I_{to}, is carried through BK channels. Apamin (100 nM), a blocker of small conductance K_{Ca} (SK) channels had no effect on either the I_{to} or I_{so} ($n = 8$). Additionally, the I_{to} was completely eliminated in a reversible manner with 10 mM TEA ($n = 4$; unpublished data). These findings, combined with the fact that the I_{to} is Ca^{2+}-sensitive, suggest that the I_{to}, similar to SMOCs, is a BK channel current activated by CICR from internal stores.

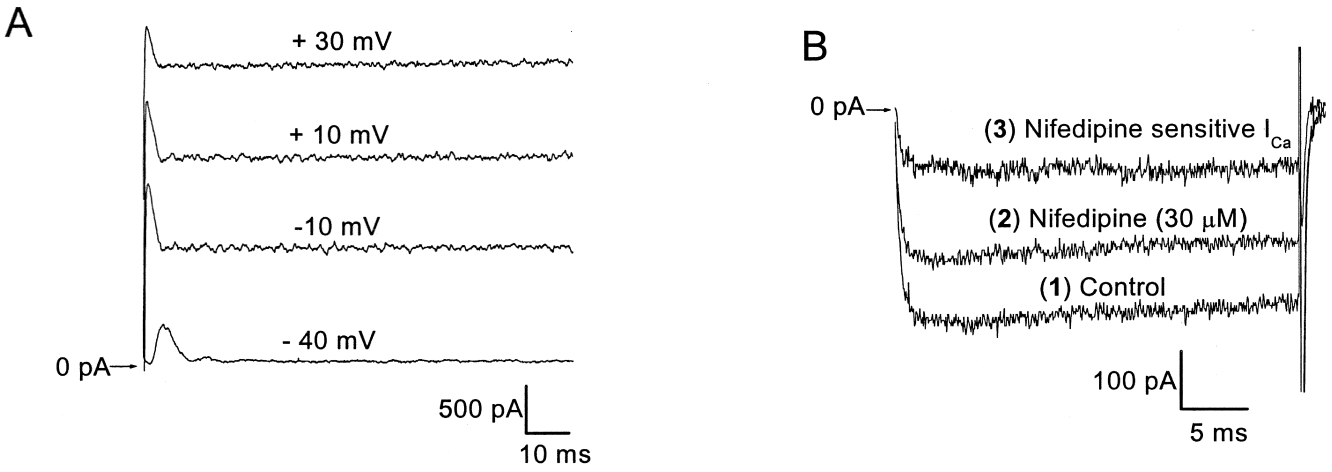

FIGURE 7. Lack of correspondence between temporal characteristics of I_{to} and the HVA Ca^{2+} current. (A) Representative recordings generated in normal Ringer's with voltage steps to −40, −10, 10, and 30 mV, showing that I_{to} decays completely within 10–15 ms after onset of the pulse. (B) Representative traces generated at 10 mV showing HVA Ca^{2+} currents. Ca^{2+} currents were isolated using 10 mM Ca^{2+}/80 mM TEA solution extracellularly and an internal solution containing 70 mM TEA. Trace 1 represents control current, 2 depicts residual current remaining after addition of 30 μM nifedipine, and 3 represents the nifedipine-sensitive current obtained by subtraction of traces 1 and 2. None of these traces shows inactivation or transient features that correspond with I_{to}.

The Ca^{2+} Influx Pathway Is not a Likely Site for the Negative Modulation of SMOCs

The earlier sections showed that increasing Ca^{2+} influx caused a temporally dependent, graded reduction in peak SMOC amplitudes. This constitutes a Ca^{2+} influx induced negative modulation of SMOCs. The disappearance of SMOCs and the concomitant appearance of the I_{to} results from a combination of increased levels of negative modulation, combined with the decreased first latency to SMOC appearance seen with increasing Ca^{2+} influx. Based on the SMOC generation pathway elucidated in the preceding paper (Mitra and Slaughter, 2002, this issue), there are three potential sites where Ca^{2+}-induced negative modulation could occur. The first candidate is the Ca^{2+} influx pathway (HVA Ca^{2+} channels), since CICR is graded with the amount of Ca^{2+} influx in a number of other cell types (Berridge, 1997). A smaller Ca^{2+} release from the stores would give rise to lower amplitude SMOCs (Bolton and Imaizumi, 1996).

HVA Ca^{2+} channels, especially the L-type, are known to exhibit voltage and Ca^{2+}-dependent inactivation (see DISCUSSION). Thus, increased influx might inactivate the calcium channel, reduce CICR, and result in the calcium- and time-dependent reduction in SMOC frequency and amplitude, eventually leading to only I_{to}. If true, there should be a correspondence between the temporal characteristics of the Ca^{2+} current and I_{to}. Fig. 7 A shows recordings of I_{to} in normal Ringer's at voltages of −40, −10, 10, and 30 mV. The I_{to} is least transient at −40 mV. However, in all cells examined, it decays completely within 15 ms. Thus, if this transient feature arises due to Ca^{2+}-induced inactivation of the HVA Ca^{2+} current, it follows that the Ca^{2+} current should show a significant degree of inactivation within this time frame. To test this possibility, recordings of HVA Ca^{2+} currents were made from cells displaying SMOCs. These currents were recorded using 10 mM [Ca^{2+}] as the charge carrier (n = 6). This would provide an influx level such that the degree of Ca^{2+}-dependent inactivation is exaggerated. Fig. 7 B shows whole cell Ca^{2+} current recordings from a representative cell with a 30 ms pulse to 10 mV. These currents do not show any significant degree of inactivation. Since it was shown in the previous paper that DHP-sensitive L-type Ca^{2+} channels are involved in the SMOC generation (Mitra and Slaughter, 2002, this issue), a dissection of the DHP-sensitive component was done. Addition of 30 μM nifedipine resulted in a parallel reduction of the control current. Nifedipine (30 μM) blocked 32 ± 3% of the control current and the effects of nifedipine were partially reversible on return to control solutions (value is an average of five cells). Since Ca^{2+} channels run down during recordings with high concentrations of Ca^{2+}, the percentage of block seen with nifedipine is probably an overestimate. Thus, the Ca^{2+} influx pathway is in all probability not the site for the Ca^{2+}-induced negative modulation of SMOCs. The other two candidates, namely the ryanodine receptors and BK channels, are also known to exhibit Ca^{2+}-induced negative feedback. However, their role was not tested in this study.

DISCUSSION

The results presented in this and the preceding paper show that retinal SMOCs exhibit a complex Ca^{2+} de-

pendence (Mitra and Slaughter, 2002, this issue). Ca^{2+} influx is a prerequisite for SMOC appearance and increases their frequency. However, higher levels of Ca^{2+} influx negatively modulate SMOCs, causing the disappearance of individual SMOCs and the appearance of the I_{to}. Thus the amount of Ca^{2+} influx into the cell determines the balance between individual SMOCs and the transient outward K^+ current, I_{to}.

Calcium-dependence of SMOC Appearance and Disappearance

In cultured mouse dorsal root ganglion cells, Mathers and Barker (1984) reported that the current variance of cells displaying SMOCs increased markedly on moving the clamp potential from −60 to −30 mV, but declined above this voltage. Thus, the authors suggested that the membrane process responsible for SMOCs is either fully activated or completely inactivated at membrane potentials positive to −20 mV. Similar to their findings, it was shown by Mitra and Slaughter (2002, this issue) that recordings in normal Ringer's from an amacrine cell subtype revealed SMOC activity within the narrow voltage window of −60 to −40 mV. Depolarizations beyond these values led to the disappearance of SMOCs. This was intriguing, since the potassium driving force should increase with depolarization, enhancing SMOC amplitudes.

Since suppression of calcium channels permitted SMOCs to appear at more positive voltages, it suggested that a Ca^{2+}-dependent factor governs not only the appearance, but also the disappearance of SMOCs. Data obtained in this and Mitra and Slaughter (2002, this issue) show that increasing Ca^{2+} influx through HVA Ca^{2+} channels increases SMOC frequency. Thus, Ca^{2+} influx up to levels that do not result in a significant degree of negative modulation are stimulatory to SMOC appearance. However, the data presented in this paper show two other notable effects of increased Ca^{2+} influx on SMOCs: both their latency and amplitudes were reduced. Extrapolating the data from experiments in the presence of cobalt to normal conditions indicates that high Ca^{2+} influx would not only reduce SMOC amplitudes, but also cause them to appear earlier, the combination of which leads to the generation of the transient outward current (I_{to}).

The mean amplitude of SMOCs was reduced in a graded manner with increasing Ca^{2+} influx. The method of analysis employed does not disclose the exact nature of this reduction. It could arise from either a lowering in amplitude of all individual SMOCs or a relatively increased appearance of small amplitude SMOCs. At high Ca^{2+} influx levels, this reduction was found to show a temporal dependence; with SMOCs generated in the latter part of the pulse displaying lower amplitudes relative to those present in the earlier part of the pulse. Since this phenomenon can be manipulated by varying extracellular calcium or by modulating the calcium channel, it is likely to represent the effects of calcium influx. The modulation of SMOC amplitude constitutes a temporally dependent Ca^{2+} influx–induced negative modulation of SMOCs.

Modulation of the Ca^{2+} influx pathway by the DHP agonist S (−) BayK 8644, or the antagonist nifedipine, gave results consistent with those obtained by manipulating $[Ca^{2+}]$. Nifedipine, though considered to be relatively selective for the L-type Ca^{2+} channel at low doses, is known to inhibit K^+ channels, especially at the high end of the range of doses used in this study (Fagni et al., 1994; Avdonin et al., 1997; Zhang et al., 1997). Since SMOCs are K^+ currents, there was a possibility that the effects of nifedipine reflected a blockade of K^+ channels rather than a reduction of Ca^{2+} influx. However, contrasting the nifedipine effect with other K^+ channel blockers such as TEA and iberiotoxin argued against this possibility. It was shown in Mitra and Slaughter (2002, this issue) that both TEA and iberiotoxin caused a graded reduction in SMOC amplitude. Thus, K^+ channel block reduces SMOC amplitude. Nifedipine, on the other hand, enhanced SMOC amplitude, suggesting an effect independent of K^+ channel block. Moreover, the reverse effect of S (−) BayK 8644 would tend to support a specific effect of these DHPs on the Ca^{2+} influx pathway.

In addition, elevated Ca^{2+} influx produced faster SMOC decay times. Although it is possible that this faster decay caused a reduction in SMOC amplitude, this may be an artifact of the measurement technique, since SMOC amplitudes were not constant under conditions of different Ca^{2+} influx. The peak-to-peak magnitude of the baseline noise could affect the measurement of SMOC parameters, such as amplitude and decay time. Although the absolute magnitude of the error in measuring amplitudes is constant for SMOCs of all amplitudes, this is not the case with the measurement of decay times. Decay time measurements of smaller SMOCs are more prone to errors that would underestimate the decay time. Since our analysis showed that smaller SMOCs were more transient, it was not possible to ensure that measurement error did not contribute to this result.

Coupled with the change in SMOC amplitude, the mean first latency to SMOC occurrence decreased as the amount of Ca^{2+} influx increased. A combination of these two Ca^{2+}-dependent phenomena resulted in SMOCs appearing sooner in response to a voltage pulse and being bigger in peak amplitude in the earlier part, while disappearing in the latter part. At relatively high levels of Ca^{2+} influx (3.6 or 4.5 mM $[Ca^{2+}]$ at 30 mV in 6 mM Co^{2+} Ringer's), an extreme consequence of these two effects was the disappearance of individual

SMOCs and the appearance of the transient outward current, I_{to}.

These observations explain the appearance of SMOCs within the narrow voltage range of −60 to −40 mV in normal Ringer's. The open probability (P_o) of HVA Ca^{2+} channels is relatively low in this hyperpolarized range (Bean, 1989). Consequently, the Ca^{2+} influx into the cell is low, a condition conducive to the appearance of discrete SMOCs. Depolarizations beyond this range would cause a greater activation of HVA Ca^{2+} channels, a greater Ca^{2+} influx, and the disappearance of discrete SMOCs, and also the concomitant appearance of the I_{to}.

Further support for this explanation comes from the pharmacological similarity between SMOCs and the I_{to}. It was shown in the preceding paper that SMOCs are Ca^{2+} influx sensitive, outward currents that are blocked by TEA and iberiotoxin. They are generated by CICR, so high doses of ryanodine or caffeine lead to their elimination (Mitra and Slaughter, 2002, this issue). Similarly, I_{to} is blocked by TEA, iberiotoxin, and high doses of ryanodine or caffeine. Thus, the I_{to}, similar to SMOCs, is generated by a process of CICR and represents K^+ fluxes through BK channels.

Site of SMOC-negative Modulation

Increasing Ca^{2+} influx leads to a temporally dependent reduction of SMOC amplitudes; this reduction constituting a Ca^{2+} influx–induced negative modulation of SMOCs. Based on the SMOC generation pathway, all three nodes (namely, the HVA Ca^{2+} channel, ryanodine receptor, or the BK channel) are potential sites, either individually or in concert, for this negative modulation.

HVA Ca^{2+} channels, such as the L-type, exhibit Ca^{2+}-dependent inactivation, in addition to pure voltage–dependent inactivation (Kass and Sanguinetti, 1984; Hadley and Hume, 1987; Kalman et al., 1988; de Leon et al., 1995). However, our experiments suggest that inactivation of the Ca^{2+} current is not a likely candidate for this negative modulation. Ca^{2+} currents were recorded under high [Ca^{2+}] (10 mM) at depolarized voltages which elicit the I_{to}. These are conditions that should accentuate Ca^{2+}-induced inactivation. Recordings of Ca^{2+} currents with 30-ms pulses (a duration in which the I_{to} is known to have fully activated and decayed) from cells showing SMOCs and the I_{to}, did not reveal significant time-dependent inactivation. Even though the L-type HVA Ca^{2+} channel is involved in SMOC generation, pharmacological isolation of the nifedipine-sensitive Ca^{2+} current did not disclose significant inactivation during this time course.

The other two potential sites are the ryanodine receptor and the BK channel. The ryanodine receptor Ca^{2+} release channel can be negatively modulated by Ca^{2+}. Biophysically, there are two distinct negative modulations of this receptor, namely Ca^{2+}-induced inactivation (Ma et al., 1988; Bezprozvanny et al., 1991; Simon et al., 1991; Percival et al., 1994; Jong et al., 1995) and adaptation of the receptor to pulses of Ca^{2+} (Gyorke and Fill, 1993; Gyorke and Palade, 1994; Gyorke et al., 1994; Yasui et al., 1994; Valdivia et al., 1995; Velez et al., 1997). Both mechanisms could potentially lead to negative modulation of SMOCs. The final potential site is the BK channel, some subtypes of which are inactivating (Pallotta, 1985; Solaro and Lingle, 1992; McLarnon, 1995; Solaro et al., 1995; Hicks and Marrion, 1998; Smith and Ashford, 2000). Solaro and Lingle (1992) reported a BK channel in rat adrenal chromaffin cells which undergoes rapid and complete inactivation. The inactivation is trypsin-sensitive and is enhanced by increased intracellular Ca^{2+} and depolarization. An examination of the above mentioned nodes might provide insights into the exact mechanism underlying the Ca^{2+} influx–induced negative modulation observed in this study.

High levels of Ca^{2+} influx might directly activate BK channels that produce the $I_{so\text{-}Ca}$. This would reduce the number of BK channels available to generate SMOCs, thus leading to a reduction in their amplitudes. However, such a mechanism would necessitate a time-dependent increase of the baseline current, since reduction of SMOC amplitudes is temporally dependent. An increase in baseline current was not observed. Thus, such a mechanism may contribute to, but not be solely responsible for, the Ca^{2+} influx–induced negative modulation of SMOCs.

Use of Inorganic Blockers to Evaluate the Voltage Dependence of SMOCs

To assess the effect of voltage on SMOC characteristics, SMOCs were generated at depolarized levels in Co^{2+} Ringer. HVA Ca^{2+} channel block by inorganic blockers such as Cd^{2+}, Co^{2+}, La^{3+}, and Mg^{2+} is concentration- and voltage-dependent, with these ions acting as pore blockers (Lansman et al., 1986; Huang et al., 1989; Winegar et al., 1991). For a positive ion sensing the membrane electric field, hyperpolarization would pull the blocker into the cell, whereas depolarizations would tend to force it out of the channel into the external solution (Woodhull, 1973; Fukushima and Hagiwara, 1985; Rosenberg and Chen, 1991; Carbone et al., 1997). Depolarization activates the HVA Ca^{2+} channel (Bean, 1989) and would also relieve the block (Thevenod and Jones, 1992; Wakamori et al., 1998; but see Byerly et al., 1984; Swandulla and Armstrong, 1989; Chow, 1991). Membrane surface charge screening by divalent ions would produce a depolarizing shift of calcium channel activation (Frankenhaeuser and Hodgkin, 1957; Hille, 1992). Both mechanisms might

be operative when divalent cations are added to reduce flux through the HVA Ca^{2+} channel. For either mechanism, a depolarizing voltage shift would result in an increase in the apparent (activated and unblocked) whole cell HVA Ca^{2+} channel conductance. The extent of Ca^{2+} influx would be governed by the product of the apparent conductance and the driving force for Ca^{2+} ions at that particular voltage.

Depolarization produces a biphasic effect on both SMOC frequency and first latency. These findings are easily explained by the underlying Ca^{2+} dependence of these parameters. Depolarization would increase the number of activated/unblocked Ca^{2+} channels, leading to an increased Ca^{2+} influx. The greater Ca^{2+} influx presumably leads to a greater success rate in triggering CICR events. This would increase SMOC frequency and decrease first latency. Further depolarization decreases the frequency and increases the first latency, presumably because the Ca^{2+} influx decreases due to reduction in the driving force for Ca^{2+} influx.

Depolarization also increased peak SMOC amplitude. As expected, the amount of K^+ current flowing through the channels should increase with depolarization. However, the gradient of the SMOC I-V profile was not linear as would be expected for a solely passive increase in current. The I-V curve had a greater slope conductance above 40 mV. A reduced Ca^{2+} influx into the cell would cause less negative modulation, and this could account for the increased slope of the SMOC I-V curve at above 40 mV. However, our experiments do not rule out the possibility of a purely voltage-dependent factor, which would increase the slope of the SMOC I-V curve at these depolarized levels.

Comparison with Muscle STOCs

Spontaneous transient outward currents (STOCs) seen in muscle cells are apparently similar to SMOCs in neurons. They too are generated by Ca^{2+} release from ryanodine-sensitive internal stores and are simultaneous activation of clusters of BK channels. There is evidence to show that the causative factor for STOCs are highly localized elevations of internal calcium ($[Ca^{2+}]_i$), called "calcium sparks" (Benham and Bolton, 1986; Nelson et al., 1995; Perez et al., 1999; ZhuGe et al., 1999). If spark-like signals were the causative factor for SMOCs, then one would expect a degree of parallelism between their properties. This may be the case, since it was shown in the previous paper that retinal SMOCs are eliminated on dialysis with 10 mM BAPTA, but not by 10 mM EGTA (Mitra and Slaughter, 2002, this issue). Merriam et al. (1999) reported a similar result in their study of SMOCs in mudpuppy parasympathetic neurons. In cardiac cells, where Ca^{2+} influx through L-type channels generates sparks via CICR, sparks have a bell-shaped frequency dependence with clamp potential. Their latency to occurrence is biphasic: decreasing initially with depolarization as the channel activated and then increasing as the current through the L-type channel decreased due to a reduction in Ca^{2+} driving force (Lopez-Lopez et al., 1995). These results are very similar to SMOCs in retinal neurons, and suggest that there may be a close analogy of underlying mechanisms in nerve and muscle cells.

Possible Physiological Significance of SMOCs

Although the physiological role of SMOCs is not clear, it may produce the slow after-hyperpolarization that follows bouts of neuronal activity (Berridge, 1998) or govern the resting membrane potential as it does in smooth muscle cells (Nelson et al., 1995). Third order neurons, amacrine and ganglion cells, are the only spiking cells in the vertebrate retina (Werblin and Dowling, 1969). These neurons exhibit spontaneous excitatory postsynaptic potentials (sEPSPs; Awatramani and Slaughter, 2001) which may reach spike threshold. This would lead to action potential propagation and transmission of information despite the absence of an external stimulus, producing a form of synaptic noise.

SMOCs result in discrete hyperpolarizations in some neurons, called SMHs (Hartzell et al., 1977; Mathers and Barker, 1981; Fletcher and Chiappinelli, 1992). Provided there is synchrony, SMHs could negate the sEPSP. Small sEPSPs, resulting in postsynaptic depolarizations of only a few millivolts, might result in SMOCs occurring with a long latency, poorly timed to counteract the sEPSPs. However, larger sEPSPs, which could potentially make the third order neuron reach action potential threshold, would trigger short latency SMOCs. The resulting SMH could potentially cancel out the sEPSP and prevent spiking. This would imply that the bigger the sEPSP, the greater the chance of an SMH being triggered in synchrony with the sEPSP. Thus, retinal SMOCs can putatively function as synaptic noise suppressors within a quiescent glutamatergic synapse. Such a noise suppression would be redundant with coordinated synaptic activity, which would also result in greater postsynaptic calcium influx; thus, the conversion of SMOCs into the I_{to}.

This work was supported by NEI grant EY05725. P. Mitra was a recipient of the Mark Diamond Research Fund award for the year 1999–2000.

Submitted: 30 July 2001
Revised: 18 March 2002
Accepted: 19 March 2002

REFERENCES

Avdonin, V., E.F. Shibata, and T. Hoshi. 1997. Dihydropyridine action on voltage-dependent potassium channels expressed in *Xenopus* oocytes. *J. Gen. Physiol.* 109:169–180.

Awatramani, G.B., and M.M. Slaughter. 2001. Intensity-dependent,

rapid activation of presynaptic metabotropic glutamate receptors at a central synapse. *J. Neurosci.* 21:741–749.

Bean, B.P. 1989. Classes of calcium channels in vertebrate cells. *Annu. Rev. Physiol.* 51:367–384.

Benham, C.D., and T.B. Bolton. 1986. Spontaneous transient outward currents in single visceral and vascular smooth muscle cells of the rabbit. *J. Physiol.* 381:385–406.

Berridge, M.J. 1997. Elementary and global aspects of calcium signalling. *J. Physiol.* 499:291–306.

Berridge, M.J. 1998. Neuronal calcium signaling. *Neuron.* 21:13–26.

Bezprozvanny, I., J. Watras, and B.E. Ehrlich. 1991. Bell-shaped calcium-response curves of $Ins(1,4,5)P_3$- and calcium-gated channels from endoplasmic reticulum of cerebellum. *Nature.* 351: 751–754.

Bolton, T.B., and Y. Imaizumi. 1996. Spontaneous transient outward currents in smooth muscle cells. *Cell Calcium.* 20:141–152.

Brown, D.A., A. Constanti, and P.R. Adams. 1983. Ca-activated potassium current in vertebrate sympathetic neurons. *Cell Calcium.* 4:407–420.

Byerly, L., P.B. Chase, and J.R. Stimers. 1984. Calcium current activation kinetics in neurones of the snail Lymnaea stagnalis. *J. Physiol.* 348:187–207.

Carbone, E., H.D. Lux, V. Carabelli, G. Aicardi, and H. Zucker. 1997. Ca^{2+} and Na^{+} permeability of high-threshold Ca^{2+} channels and their voltage-dependent block by Mg^{2+} ions in chick sensory neurones. *J. Physiol.* 504:1–15.

Chow, R.H. 1991. Cadmium block of squid calcium currents. Macroscopic data and a kinetic model. *J. Gen. Physiol.* 98:751–770.

de Leon, M., Y. Wang, L. Jones, E. Perez-Reyes, X. Wei, T.W. Soong, T.P. Snutch, and D.T. Yue. 1995. Essential Ca^{2+}-binding motif for Ca^{2+}-sensitive inactivation of L-type Ca^{2+} channels. *Science.* 270: 1502–1506.

Fagni, L., J.L. Bossu, and J. Bockaert. 1994. Inhibitory effects of dihydropyridines on macroscopic K^{+} currents and on the large-conductance Ca^{2+}-activated K^{+} channel in cultured cerebellar granule cells. *Pflugers Arch.* 429:176–182.

Fletcher, G.H., and V.A. Chiappinelli. 1992. Spontaneous miniature hyperpolarizations of presynaptic nerve terminals in the chick ciliary ganglion. *Brain Res.* 579:165–168.

Frankenhaeuser, B., and A.L. Hodgkin. 1957. The action of calcium on the electrical properties of squid axons. *J. Physiol.* 137: 218–244.

Fukushima, Y., and S. Hagiwara. 1985. Currents carried by monovalent cations through calcium channels in mouse neoplastic B lymphocytes. *J. Physiol.* 358:255–284.

Gyorke, S., and M. Fill. 1993. Ryanodine receptor adaptation: control mechanism of Ca^{2+}-induced Ca^{2+} release in heart. *Science.* 260:807–809.

Gyorke, S., and P. Palade. 1994. Ca^{2+}-dependent negative control mechanism for Ca^{2+}-induced Ca^{2+} release in crayfish muscle. *J. Physiol.* 476:315–322.

Gyorke, S., P. Velez, B. Suarez-Isla, and M. Fill. 1994. Activation of single cardiac and skeletal ryanodine receptor channels by flash photolysis of caged Ca^{2+}. *Biophys. J.* 66:1879–1886.

Hadley, R.W., and J.R. Hume. 1987. An intrinsic potential-dependent inactivation mechanism associated with calcium channels in guinea-pig myocytes. *J. Physiol.* 389:205–222.

Hartzell, H.C., S.W. Kuffler, R. Stickgold, and D. Yoshikami. 1977. Synaptic excitation and inhibition resulting from direct action of acetylcholine on two types of chemoreceptors on individual amphibian parasympathetic neurones. *J. Physiol.* 271:817–846.

Hicks, G.A., and N.V. Marrion. 1998. Ca^{2+}-dependent inactivation of large conductance Ca^{2+}-activated K^{+} (BK) channels in rat hippocampal neurones produced by pore block from an associated particle. *J. Physiol.* 508:721–734.

Hille, B. 1992. Ionic Channels in Excitable Membranes. 2nd ed. Sinauer Associates, Inc. Sunderland, MA. 607 pp.

Huang, Y., J.M. Quayle, J.F. Worley, N.B. Standen, and M.T. Nelson. 1989. External cadmium and internal calcium block of single calcium channels in smooth muscle cells from rabbit mesenteric artery. *Biophys. J.* 56:1023–1028.

Jong, D.S., P.C. Pape, S.M. Baylor, and W.K. Chandler. 1995. Calcium inactivation of calcium release in frog cut muscle fibers that contain millimolar EGTA or Fura-2. *J. Gen. Physiol.* 106:337–388.

Kalman, D., P.H. O'Lague, C. Erxleben, and D.L. Armstrong. 1988. Calcium-dependent inactivation of the dihydropyridine-sensitive calcium channels in GH3 cells. *J. Gen. Physiol.* 92:531–548.

Kass, R.S., and M.C. Sanguinetti. 1984. Inactivation of calcium channel current in the calf cardiac Purkinje fiber. Evidence for voltage- and calcium-mediated mechanisms. *J. Gen. Physiol.* 84: 705–726.

Lansman, J.B., P. Hess, and R.W. Tsien. 1986. Blockade of current through single calcium channels by Cd^{2+}, Mg^{2+}, and Ca^{2+}. Voltage and concentration dependence of calcium entry into the pore. *J. Gen. Physiol.* 88:321–347.

Lopez-Lopez, J.R., P.S. Shacklock, C.W. Balke, and W.G. Wier. 1995. Local calcium transients triggered by single L-type calcium channel currents in cardiac cells. *Science.* 268:1042–1045.

Ma, J., M. Fill, C.M. Knudson, K.P. Campbell, and R. Coronado. 1988. Ryanodine receptor of skeletal muscle is a gap junction-type channel. *Science.* 242:99–102.

Mathers, D.A., and J.L. Barker. 1981. Spontaneous hyperpolarizations at the membrane of cultured mouse dorsal root ganglion cells. *Brain Res.* 211:451–455.

Mathers, D.A., and J.L. Barker. 1984. Spontaneous voltage and current fluctuations in tissue cultured mouse dorsal root ganglion cells. *Brain Res.* 293:35–47.

McLarnon, J.G. 1995. Inactivation of a high conductance calcium dependent potassium current in rat hippocampal neurons. *Neurosci. Lett.* 193:5–8.

Merriam, L.A., F.S. Scornik, and R.L. Parsons. 1999. Ca^{2+}-induced Ca^{2+} release activates spontaneous miniature outward currents (SMOCs) in parasympathetic cardiac neurons. *J. Neurophysiol.* 82: 540–550.

Mitra, P., and M. Slaughter. 2000. Low calcium influx induced potassium current spikes in retinal third order neurons. *Invest. Ophthalmol. Vis. Sci.* 41:S618.

Mitra, P., and M.M. Slaughter. 2002. Mechanism of generation of spontaneous miniature outward currents (SMOCs) in retinal amacrine cells. *J. Gen. Physiol.* 119:355–372.

Nelson, M.T., H. Cheng, M. Rubart, L.F. Santana, A.D. Bonev, H.J. Knot, and W.J. Lederer. 1995. Relaxation of arterial smooth muscle by calcium sparks. *Science.* 270:633–637.

Nerbonne, J.M., and A.M. Gurney. 1987. Blockade of Ca^{2+} and K^{+} currents in bag cell neurons of *Aplysia californica* by dihydropyridine Ca^{2+} antagonists. *J. Neurosci.* 7:882–893.

Pallotta, B.S. 1985. Calcium-activated potassium channels in rat muscle inactivate from a short-duration open state. *J. Physiol.* 363: 501–516.

Pang, D.C., and N. Sperelakis. 1984. Uptake of calcium antagonistic drugs into muscles as related to their lipid solubilities. *Biochem. Pharmacol.* 33:821–826.

Percival, A.L., A.J. Williams, J.L. Kenyon, M.M. Grinsell, J.A. Airey, and J.L. Sutko. 1994. Chicken skeletal muscle ryanodine receptor isoforms: ion channel properties. *Biophys. J.* 67:1834–1850.

Perez, G.J., A.D. Bonev, J.B. Patlak, and M.T. Nelson. 1999. Functional coupling of ryanodine receptors to KCa channels in smooth muscle cells from rat cerebral arteries. *J. Gen. Physiol.* 113:229–238.

Reiser, M.A., T. D'Souza, and S.E. Dryer. 1996. Effects of caffeine

and 3-isobutyl-1-methylxanthine on voltage-activated potassium currents in vertebrate neurones and secretory cells. *Br. J. Pharmacol.* 118:2145–2151.

Rosenberg, R.L., and X.H. Chen. 1991. Characterization and localization of two ion-binding sites within the pore of cardiac L-type calcium channels. *J. Gen. Physiol.* 97:1207–1225.

Satin, L.S., and P.R. Adams. 1987. Spontaneous miniature outward currents in cultured bullfrog neurons. *Brain Res.* 401:331–339.

Simon, B.J., M.G. Klein, and M.F. Schneider. 1991. Calcium dependence of inactivation of calcium release from the sarcoplasmic reticulum in skeletal muscle fibers. *J. Gen. Physiol.* 97:437–471.

Smith, M.A., and M.L. Ashford. 2000. Inactivation of large-conductance, calcium-activated potassium channels in rat cortical neurons. *Neuroscience.* 95:33–50.

Solaro, C.R., and C.J. Lingle. 1992. Trypsin-sensitive, rapid inactivation of a calcium-activated potassium channel. *Science.* 257:1694–1698.

Solaro, C.R., M. Prakriya, J.P. Ding, and C.J. Lingle. 1995. Inactivating and noninactivating Ca^{2+}- and voltage-dependent K^+ current in rat adrenal chromaffin cells. *J. Neurosci.* 15:6110–6123.

Swandulla, D., and C.M. Armstrong. 1989. Calcium channel block by cadmium in chicken sensory neurons. *Proc. Natl. Acad. Sci. USA.* 86:1736–1740.

Thevenod, F., and S.W. Jones. 1992. Cadmium block of calcium current in frog sympathetic neurons. *Biophys. J.* 63:162–168.

Valdivia, H.H., J.H. Kaplan, G.C. Ellis-Davies, and W.J. Lederer. 1995. Rapid adaptation of cardiac ryanodine receptors: modulation by Mg^{2+} and phosphorylation. *Science.* 267:1997–2000.

Velez, P., S. Gyorke, A.L. Escobar, J. Vergara, and M. Fill. 1997. Adaptation of single cardiac ryanodine receptor channels. *Biophys. J.* 72:691–697.

Wakamori, M., M. Strobeck, T. Niidome, T. Teramoto, K. Imoto, and Y. Mori. 1998. Functional characterization of ion permeation pathway in the N-type Ca^{2+} channel. *J. Neurophysiol.* 79:622–634.

Werblin, F.S., and J.E. Dowling. 1969. Organization of the retina of the mudpuppy, Necturus maculosus. II. Intracellular recording. *J. Neurophysiol.* 32:339–355.

Winegar, B.D., R. Kelly, and J.B. Lansman. 1991. Block of current through single calcium channels by Fe, Co, and Ni. Location of the transition metal binding site in the pore. *J. Gen. Physiol.* 97: 351–367.

Woodhull, A.M. 1973. Ionic blockage of sodium channels in nerve. *J. Gen. Physiol.* 61:687–708.

Yasui, K., P. Palade, and S. Gyorke. 1994. Negative control mechanism with features of adaptation controls Ca^{2+} release in cardiac myocytes. *Biophys. J.* 67:457–460.

Zhang, X., J.W. Anderson, and D. Fedida. 1997. Characterization of nifedipine block of the human heart delayed rectifier, hKv1.5. *J. Pharmacol. Exp. Ther.* 281:1247–1256.

ZhuGe, R., R.A. Tuft, K.E. Fogarty, K. Bellve, F.S. Fay, and J.V. Walsh, Jr. 1999. The influence of sarcoplasmic reticulum Ca^{2+} concentration on Ca^{2+} sparks and spontaneous transient outward currents in single smooth muscle cells. *J. Gen. Physiol.* 113: 215–228.